EPR of Gd^{3+} in Sulfate Host Crystals of Low Symmetry

M. Bode, B. D. Mosel, and W. Müller-Warmuth

Institut für Physikalische Chemie der Westfälischen Wilhelms-Universität Münster, D-48149 Münster

Z. Naturforsch. **52a**, 323–330 (1997); received December 16, 1996

Electron paramagnetic resonance (EPR) spectra of trivalent gadolinium have been investigated in orthorhombic sulfate host crystals $MeSO_4$ with Me = Sr, Ba, Cd, Hg, Pb and K_2SO_4. Because of the low symmetry of the host crystals and the spin quantum number 7/2, complex spectra for several orientations of the magnetic field containing a large number of individual lines had to be analyzed. The spin Hamiltonian parameters have been rigorously determined from the rotational diagrams. Gd^{3+} has been found to substitute, first of all, for the monoclinic sites of the host metal ion with charge compensation at larger distances. To a small extent, charge compensation in the vicinity has also been observed, arising from additional centres and spectra with lower intensities. Correlations between EPR spectra and crystal structure are reflected in the values of the zero field splitting parameters.

1. Introduction

Electron paramagnetic resonance (EPR) spectroscopy of transition metal or rare earth ions in diamagnetic host crystals is a powerful technique to study local structures and to probe crystalline electric fields. Based on the splitting of groundstates in magnetic and crystalline electric fields, EPR displays in particular zero field splitting (ZFS) information which depends greatly on the environment and site symmetry of the paramagnetic guest. Size and sign of the ZFS parameters cover a large range depending sensitively on the details of the particular system.

Trivalent gadolinium guest ions in diamagnetic crystals are of both scientific and technological interest, for instance in LASER materials. Gd^{3+} has seven unpaired electrons with total spin $S = 7/2$ and a $^8S_{7/2}$ groundstate. EPR spectra are therefore distinguished by a large number of individual transitions. Most studies have so far been made on Gd^{3+} guest ions incorporated in highly symmetric crystals, at least with tetragonal structure. In host crystals with low symmetry, a still larger number of signals has to be expected and the analysis of the complex spectra means a particular challenge for the spectroscopist. To our knowledge, to date no EPR measurements on Gd^{3+} in orthorhombic sulfates $MeSO_4$ with Me = Sr, Ba, Cd, Hg, and Pb or K_2SO_4 have been reported. All these compounds show orthorhombic crystal structure with a monoclinic site symmetry of the metal ion; single crystal spectra for several orientations of the magnetic field are required. Powder spectra can only be used for determining the spin Hamiltonian parameters in exceptional cases if some information on the site symmetry is already available.

In this purpose of this study to determine the spin Hamiltonian parameters rigorously by least-squares computer fitting procedures and diagonalizing the matrix. A large number of resonances measured for several orientations of the crystals in the magnetic field was to be evaluated during the fitting procedure. From the spin Hamiltonian parameters, especially from the ZFS, information such as incorporation of the paramagnetic ions, defect structure, symmetry of various centres and charge compensation mechanisms was expected. The experimental procedures were similar to those in two preceding papers on EPR of Tb^{4+} in host crystals with zircon structure [1] and of Cr^{3+} and Fe^{3+} in langbeinites [2].

Reprint requests to Prof. W. Müller-Warmuth,
Fax: 02 51 8 32 34 41.

2. Experimental Details

2.1 Sample Preparation

Single crystals of the sulfates $MeSO_4$ with Me = Ba^{2+}, Sr^{2+}, Cd^{2+}, and Hg^{2+} were grown in our laboratory by dissolving the compounds together with 0.2–2 mol% of the dopant ion Gd^{3+} in hot concentrated sulfuric acid and by evaporating the solution to dryness at 200 °C over a period of three to seven days. By the evaporation single crystals of sufficient size and quality for the EPR measurements were produced.

0932-0784 / 97 / 0400-0323 $ 06.00 © – Verlag der Zeitschrift für Naturforschung, D-72072 Tübingen

Gadolinium doped $PbSO_4$ could be obtained as a powder by the flux method as already described in the literature [3–5]. But $PbSO_4$:Gd^{3+} could also be prepared by coprecipitation of a diluted aqueous $PbNO_3$ solution with diluted H_2SO_4 in the presence of 10 mol% Gd^{3+} ions.

Single crystals of gadolinium doped K_2SO_4 were obtained by slow evaporation from aqueous solution over seven to ten days in the presence of 0.5 mol% Gd^{3+}.

2.2 Crystal Structure

All samples showed an orthorhombic crystal structure with the metal ion occupying a monoclinic site. The space groups are Pnma (no. 62 using the *Schönfließ* notation) for the isomorphous sulfates of Ba, Sr, Pb with four crystallographic identical metal ions per unit cell [6, 7], $Pn2_1m$ (no. 31) for the isomorphous sulfates of Cd and Hg with two crystallographically identical metal ions per unit cell [8] and Pnam (no. 62) for K_2SO_4 with two groups of two crystallographically identical K^+-ions each, denoted by α and β [9]. The monoclinic axes perpendicular to a mirror plane, which is the highest symmetry element in these crystal structures, are the *b*-axis (Ba, Sr, Pb) and the *c*-axis (Cd, Hg, K), respectively.

2.3 EPR Spectroscopy

The EPR data were collected on a conventional Bruker ESP 300 X-Band (9–10 GHz) spectrometer. Temperature dependent measurements down to 77 K were made by applying a liquid nitrogen flux system. For measurements at 77 K a liquid nitrogen quartz dewar was used and below 77 K a closed cyclic Helium cryostat.

Measurements of the magnetic field strength were made using a proton NMR gaussmeter while either a picein standard sample ($g = 2.0041$ (1)) [10] or an electronic microwave frequency controller was used to determine the X-band microwave frequency.

The single crystal samples were mounted on a quartz glass rod and could be rotated around their magnetic axes which proved to be not identical with their crystallographic axes. Detailed measurements of the angular dependence of the spectrum were carried out in steps of 2°, whereas the simulations were calculated in 1° steps.

2.4 Data Analysis

Gd^{3+} has a $4f^7$ configuration with a $^8S_{7/2}$ free-ion groundstate and 8-fold degeneracies. From group theoretical considerations it can be infered that Gd^{3+} ions in crystal fields of monoclinic symmetry have the free ion ground state split into four Kramers doublets even in the absence of a magnetic field. A magnetic field leads to the removal of the twofold degeneracy and splits the Kramers doublets into eight Zeeman levels which lead to seven observed EPR transitions in the spectrum (Figure 1). Using homemade programs, the spectra could be fitted to the monoclinic spin Hamiltonian [11]

$$\hat{\mathcal{H}} = \mu_B \boldsymbol{B}_0 \tilde{g} \hat{\boldsymbol{S}} + \sum_{n=2}^{2S} \sum_{m=-n}^{n} B_n^m \mathbf{O}_n^m \qquad (1)$$

with an effective electronic spin $\hat{\boldsymbol{S}}$ of 7/2, the Bohr Magneton μ_B, the Stevens Operators $\mathbf{O}_n^m$ and the ZFS parameters B_n^m, which were determined experimentally ($m \leq n$; $\mathbf{O}_0^0$ shifts all terms equally and does not need to be considered; terms with odd n disappear due to time reversal symmetry).

3. Results

The rotational diagrams of all substances revealed monoclinic spectra, a fact which is indicated by the appearance of two symmetry spectra due to two magnetically inequivalent sites of Gd^{3+}. The magnetic principal axes system, defined as z, y, x in order of decreasing crystal field splitting, and the crystallographic axes system a, b, c do not coincide. Only one magnetic and one crystallographic axis coincides, whereas the other axes lying in the same plane are twisted around a certain angle.

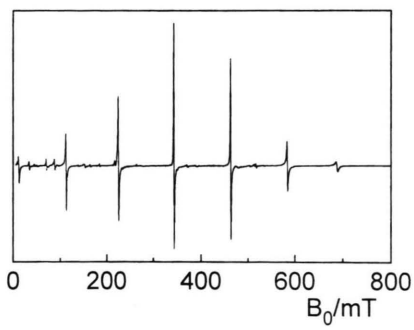

Fig. 1. Single crystal EPR spectrum of $BaSO_4$:Gd^{3+} with $B_0 \parallel z$ measured at 9.57 GHz and 40 K.

Table 1. Zero field splitting (ZFS) parameters of Gd^{3+} in the various host crystals derived from single crystal EPR spectra. The Eulerian angles describe the location of the magnetic principal axes (x, y, z) of Gd^{3+} in the crystal (a, b, c).

	$BaSO_4$					$SrSO_4$	$CdSO_4$		$HgSO_4$		K_2SO_4 (I)	K_2SO_4 (II)
T/K	298	100	77	50	30	298	298	77	298	77	298	298
ψ/Grad	90.0(0)	−95.1(9)	−95.1(7)	−92.2(0)	−96.7(4)	90.0(0)	0.0(0)	0.0(0)	0.0(0)	90.0(0)	37.2(1)	−34.8(1)
θ/Grad	90.0(0)	−90.4(0)	−90.4(3)	−88.6(4)	−89.8(2)	90.0(0)	45.0(0)	45.0(0)	45.0(0)	45.0(0)	0.0(0)	0.0(0)
ϕ/Grad	−82.9(1)	32.0(2)	32.0(4)	31.8(7)	30.6(1)	−59.4(2)	0.0(0)	0.0(0)	0.0(0)	−90.0(0)	0.0(0)	0.0(0)
B_2^0/GHz	0.507(4)	0.532(0)	0.533(5)	0.539(2)	0.538(2)	0.534(2)	0.753(1)	0.800(9)	−0.587(9)	−0.636(2)	−0.493(3)	−0.493(3)
B_2^2/GHz	0.293(9)	0.265(0)	0.262(3)	0.259(6)	0.2545	0.369(4)	0.192(4)	0.121(9)	−0.048(9)	−0.047(5)	−0.431(6)	−0.422(5)
B_2^{-2}/GHz	−0.026(9)	−0.027(8)	−0.0302(2)	−0.036(2)	−0.038(1)	−0.017(6)	−0.004(6)	−0.270(3)	0.000(1)	−0.000(9)	−0.035(6)	−0.011(4)
$B_4^0/10^{-3}$ GHz	−0.235(0)	−0.234(5)	−0.235(7)	−0.219(4)	−0.346(8)	−0.166(0)	0.206(1)	0.270(3)	−0.209(6)	−0.341(8)	−0.317(5)	0.086(4)
$B_4^2/10^{-3}$ GHz	−1.042(0)	−1.237(4)	−1.300(2)	−1.337(8)	−1.113(0)	0.313(0)	0.177(4)	1.965(5)	−2.050(0)	2.080(6)	−0.175(2)	−0.066(8)
$B_4^{-2}/10^{-3}$ GHz	0.583(0)	0.579(9)	0.569(2)	0.480(4)	1.099(7)	−1.093(0)	0.120(3)	−0.050(4)	−0.119(9)	0.011(8)	−0.346(1)	−0.889(7)
$B_4^4/10^{-3}$ GHz	−0.593(0)	−0.640(0)	−0.680(2)	−0.819(3)	0.130(1)	0.943(7)	−0.470(7)	−0.879(2)	0.659(9)	0.928(5)	1.425(4)	0.326(4)
$B_4^{-4}/10^{-3}$ GHz	0.863(0)	1.072(7)	1.069(6)	1.139(6)	1.424(6)	0.473(0)	0.001(5)	0.065(2)	0.099(7)	−0.061(4)	−3.627(5)	3.339(7)

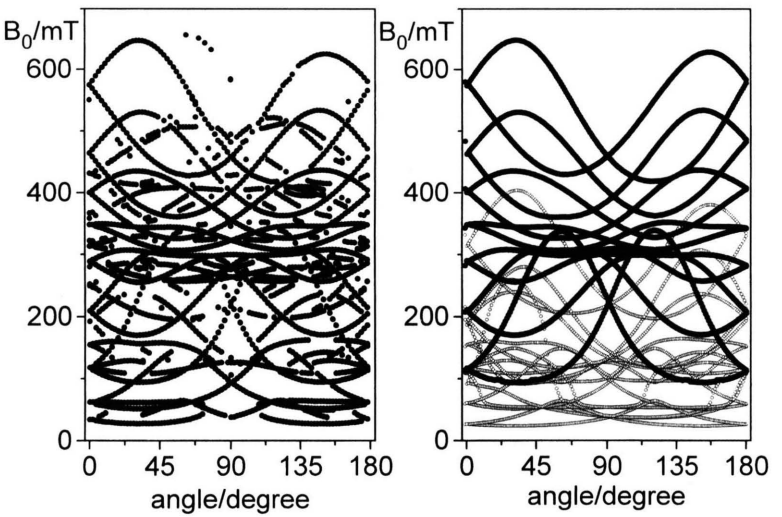

Fig. 2. Measured (left) and simulated (right) rotational diagrams of $SrSO_4$: Gd^{3+} at 9.80 GHz and 298 K. The crystal is rotated about b and z, respectively, covering the magnetic y and x axes. The small points in the simulation (right) belong to forbidden transitions with $\Delta m_s > \pm 1$.

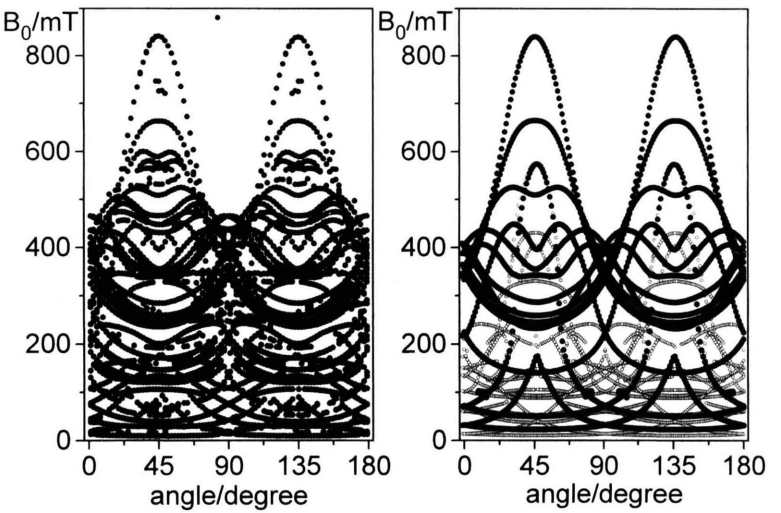

Fig. 4. Measured (left) and simulated (right) rotational diagrams of $CdSO_4$: Gd^{3+} at 9.80 GHz and 298 K. The crystal is rotated about c and y, respectively, covering the magnetic z and x axes. The small points in the simulation (right) belong to forbidden transitions with $\Delta m_s > \pm 1$.

As usual, the hyperfine structure of the two gadolinium isotopes ^{155}Gd and ^{157}Gd (both $I = 3/2$) could not be detected in the spectra. The g values of all compounds proved to be nearly isotropic with $g = 1.99$; they are therefore not listed explicitly in the following tables which present the results.

The orientation of the magnetic axes in the laboratory system, i.e., the axis system of the applied magnetic field, is described by Eulerian angles. The first angle rotates the sytem about the z axis, the second are about the new y axis and the third one about the new z axis.

The spin-Hamiltonian parameters B_6^m are smaller than the precision of the computing. The other constants B_2^m and B_4^m were accurately determined. They are presented in Table 1 together with the measured Eulerian angles.

3.1 $BaSO_4:Gd^{3+}$, $SrSO_4:Gd^{3+}$

Rotational diagrams of both substances were measured about three crystallographic axes. A representative single crystal spectrum for a fixed orientation $\boldsymbol{B}_0$ nearly parallel to the magnetic z axis is shown in Figure 1. A rotation of the crystal about the crystallographic b axis, which is in this case the monoclinic axis and which coincides with the magnetic z axis, is shown in Figure 2. The angle between the x and the a axis in the plane is nearly 7° for $BaSO_4:Gd^{3+}$ and 30° for $SrSO_4:Gd^{3+}$. Two symmetry spectra are clearly recognizable and the zero field splitting is small compared with the Zeeman splitting. The absolute sign of the ZFS was determined by low temperature measurements at a fixed orientation of the crystal. Then, the relative intensities of the signals at high magnetic field increase more than the intensities of the signals at low magnetic field (see example spectrum in Figure 1). This experiment indicates a positive sign of the ZFS parameters. In addition, rotational diagrams of $BaSO_4:Gd^{3+}$ and powder spectra of $SrSO_4:Gd^{3+}$ at low temperatures were measured. The ZFS of $BaSO_4:Gd^{3+}$ increases linearly with decreasing temperature, that of $SrSO_4:Gd^{3+}$ remains nearly constant (Table 2). The axial distortion of the trivalent gadolinium site, defined by the ratio B_2^0/B_2^2, increases for $BaSO_4:Gd^{3+}$ and decreases for $SrSO_4:Gd^{3+}$ with decreasing temperature.

Table 2. Dominant ZFS parameters of Gd^{3+} in host crystals of $SrSO_4$ and $PbSO_4$ as obtained from EPR powder spectra.

	$PbSO_4$	
T/K	298	77
B_2^0/GHz	0.476(6)	0.503(1)
B_2^2/GHz	0.202(5)	0.189(6)

	$SrSO_4$					
T/K	298	250	200	150	100	35
B_2^0/GHz	0.534(2)	0.533(4)	0.533(6)	0.535(4)	0.537(0)	0.539(9)
B_2^2/GHz	0.369(4)	0.373(2)	0.385(1)	0.288(2)	0.397(8)	0.408(8)

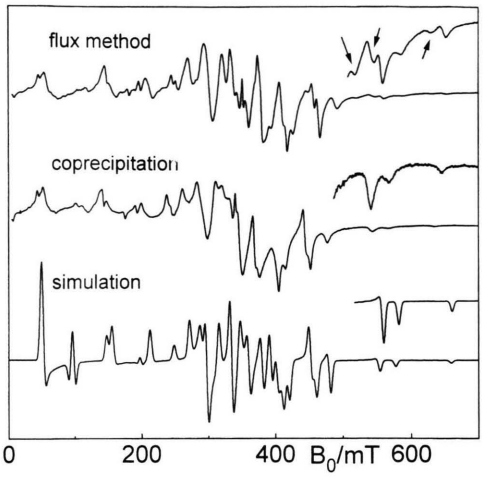

Fig. 3. Powder EPR spectra of $PbSO_4:Gd^{3+}$, prepared by the flux method and by coprecipitation at 9.76 GHz and 298 K and the simulated spectrum at the bottom. The arrows in the expanded high field part of the flux spectrum indicate signals which do not appear in the coprecipitation spectrum.

3.2 $PbSO_4:Gd^{3+}$

Powder spectra of $PbSO_4:Gd^{3+}$ prepared by the flux method and by coprecipitation are shown in Figure 3. Both spectra are very similar, only in the high field region certain differences appear. The flux product shows additional signals of lower intensity indicated by arrows in Fig. 3, which stem from extra Gd^{3+} centers with triclinic symmetry. Due to the excess of Na^+ ions during the preparation, in this case Na^+ is incorporated in the crystal in the vicinity of Gd^{3+} and lowers the symmetry of the Gd^{3+} site. This yields additional Gd^{3+} centers with different zero field splittings. From the low intensity of these signals it can be concluded that there is no strong tendency to form Gd^{3+}-Na^+ centers due to charge compensation. At 77 K the ZFS increases slightly (cf. Table 1), and the axial distortion decreases as described in the previous section for the Ba and Sr sulfates.

3.3 $CdSO_4:Gd^{3+}$, $HgSO_4:Gd^{3+}$

For $CdSO_4:Gd^{3+}$ and $HgSO_4:Gd^{3+}$ the orientation of the magnetic axes in the crystal is identical. The crystallographic c and the magnetic y axes coincide and the magnetic z and x axes are 45° apart from the a and b axes in the plane. Therefore, the magnetic z axis of the first symmetry spectrum and the x'' axis of the second symmetry spectrum coincide, and two equal maxima appear in the rotational diagrams during a rotation of the crystal about c and y, respectively (Figure 4). The extra signals in the measurement are produced by Gd^{3+} with a triclinic surrounding. Here the ZFS is not small in comparison with the Zeeman splitting so that eight instead of seven allowed signals appear in the spectra.

The absolute sign of the ZFS is positive for $CdSO_4:Gd^{3+}$ and negative for $HgSO_4:Gd^{3+}$ which could be concluded from the relative signal intensities in the temperature range down to 77 K. The signal positions vary linearly with temperature in this range. The axial character of the Gd^{3+}-site, which is described by the ratio B_2^0/B_2^2, increases strongly for $CdSO_4:Gd^{3+}$,whereas for $HgSO_4:Gd^{3+}$ it remains nearly unchanged in the temperature range from 298 K to 77 K. The equatorial ZFS parameter B_2^2 for $HgSO_4:Gd^{3+}$ is very small compared with the axial parameter B_2^0. Therefore, it can be concluded that the immediate surrounding of the Gd^{3+} site in $HgSO_4:Gd^{3+}$ is nearly axial symmetric.

The magnetic x and y axis in $HgSO_4:Gd^{3+}$ exchange their positions when lowering the temperature. At room temperature the z and x'' axes coincide whereas at 77 K the z and y'' axes coincide (Eulerian angles in Table 1). At 295 K the x and y axis are identical and Gd^{3+} is ideally axially surrounded by its ligands. This could be concluded from powder measurements at low temperatures and pursuing the signal positions of a selected x and y signal, which coincide at 259 K into one (Figure 5).

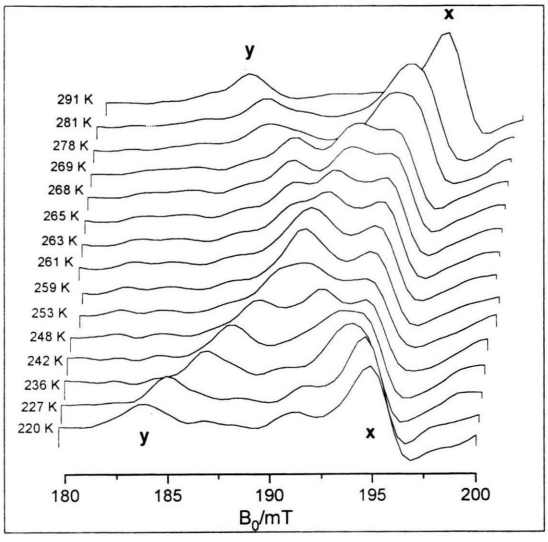

Fig. 5. Temperature dependent powder EPR spectra of $HgSO_4:Gd^{3+}$ (detail from the low field part of the spectrum) at 9.33 GHz; y and x denote the splitting of the corresponding magnetic axes.

3.4 $K_2SO_4:Gd^{3+}$

The α and β K^+ sites are equally occupied by Gd^{3+} ions. Each of the two crystallographically non-identical K^+ sites contains two magnetically non-identical Gd^{3+}. As a result, instead of seven expected signals four times as much signals appear. In the spectra, the axial ZFS parameter B_2^0 is identical for both crystallographic sites, whereas the equatorial parameter B_2^2 differs. This means, that the axial distortion of the nearest ligand surrounding for Gd^{3+} on both K^+-sites is identical, but not the equatorial distortion. The positions of the magnetic axes in the crystal differ as well. The magnetic y axis is the monoclinic axis and coincides with the crystallographic c axis. The z axis forms an angle of 37° and −34°, respectively, with the crystallographic a axis. The similarity of the α and β K^+ sites makes a definite assignment of the two Gd^{3+} centers to one K^+ site impossible.

The absolute sign of the ZFS is negative, as determined from measurements at temperatures down to 100 K. With decreasing temperature the spectra exhibit a linear spreading. No discontinuity and hence no phase transition, as reported in [12], could be detected in the temperature region from 298 K to 100 K.

4. Discussion

4.1 Incorporation of Gd^{3+}

Trivalent gadolinium substitutes in all samples for the divalent and monovalent metal ion, respectively. This can be concluded from the appearance of two symmetry spectra in the rotational diagrams due to

two magnetically inequivalent gadolinium sites. This indicates in an orthorhombic crystal lattice a monoclinic site of the impurity ion [13], and the only monoclinic site here is the site of the host metal ion.

The location of the principal axes system of the Gd^{3+} ions in the crystal lattice was also obtained. One axis coincides with the monoclinic axis of preference, i.e., $y \parallel c$ for $CdSO_4$, $HgSO_4$ and K_2SO_4 and $z \parallel b$ for $SrSO_4$ and $BaSO_4$. The other two magnetic axes lie in the plane perpendicular to this direction. They appear twice, mirrored about the crystal axes. We observe therefore two symmetry spectra resulting from two non-equivalent gadolinium centres of identical (crystal) symmetry.

The principal axes for the g tensor and the hyperfine splitting (not discussed) are the same as those for the ZFS.

4.2 Charge Compensation

For trivalent gadolinium at divalent or monovalent sites charge compensation is required. The charge compensation for the main gadolinium centre cannot take place in the immediate vicinity of the impurity ion. This would lead to a strong local distortion of the lattice in conjunction with the disappearance of the mirror plane. In this case, the symmetry would be lowered to triclinic and the spectra would change drastically. Hence, the charge compensation has to take place at larger distances. Charge compensation in the immediate vicinity was also found, but to a lesser extent; it leads to several additional centres with lower intensity which could be observed in some of the spectra.

In principle, the following mechanisms for charge compensation are imaginable:

i) hydrogen sulfate or sulfate ions could be incorporated at interstitial sites. Assuming a spherical geometry for the sulfate and the hydrogen sulfate, respectively, with an S–O-distance of 140 to 150 pm in all described sulfates, the anions are 2 to 2.5 times bigger than the host ion and the impurity ion, respectively. The incorporation of such a big ion seems rather improbable due to local lattice relaxations.

ii) The incorporation of a proton on a metal ion site, on principle conceivable by sample preparation from concentrated sulfuric acid, seems similarly improbable, again due to the extreme lattice relaxation.

iii) Imaginable is also the incorporation of small cations at the site of the metal ion. Only the flux method provides a sufficiently high concentration of monovalent cations. Indeed $PbSO_4:Gd^{3+}$, if prepared by the flux method, showed additional Gd^{3+} centres which did not appear in samples prepared by coprecipitation.

iv) Most likely, except for samples prepared by the flux method, cation vacancies seem to be responsible as already proposed by several authors [14–16].

4.3 Temperature Dependence

Since no phase transitions were observed, the temperature effects are essentially confined to small variations of the ZFS parameters, cf. Tables 1 and 2. The dominant parameter $|B_2^0|$ increases for all compounds upon decreasing temperature. This is connected with an increase of the total width of the EPR spectra. Most other ZFS parameters display only rather small and non-systematic dependences on temperature.

Distinction between implicit effects on the parameters caused by the influence of the temperature on the volume of the crystal, and explicit effects by the interaction of the electronic groundstate with excited states via lattice vibrations [17], is not possible, though implicit effects would explain the tendency of the changes of B_2^0. But explicit effects may have a similar influence.

A measure of the axial distortion and therefore of the immediate ligand environment is B_2^0/B_2^2. If the lattice contraction would be the same for all investigated materials, this ratio was expected to change in the same way. This is, however, not the case. Upon decreasing the temperature from 298 K to 77 K, for $BaSO_4$, $HgSO_4$ and $PbSO_4$ host crystals the ratio increases up to 15%, for $CdSO_4$ this increase amounts to 70%, whereas for $SrSO_4$ there is a decrease of about 8%.

4.4 Correlation of EPR Data and Crystal Structure

The most remarkable correlation between EPR data and crystal structure is found between the absolute values of the dominant ZFS parameters $|B_2^0|$ and $|B_2^2|$ and the mean metal-oxygen distances in the lattices as shown in Figure 6. The parameter $|B_2^0|$ decreases with r_{MeO}, whereas $|B_2^2|$ increases. For $|B_2^0|$ this can be interpreted in terms of the crystal field strength: a decreasing mean ligand distance increases

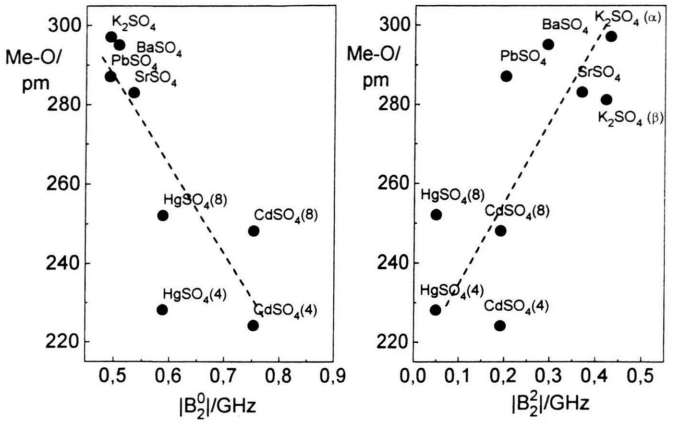

Fig. 6. ZFS parameters $|B_2^0|$ and $|B_2^2|$ at 298 K plotted versus the mean metal-ligand distances of the first ligand sphere. (4) and (8) means four and eight-coordination, alternatively, whereas (α) and (β) denote the two K^+ centers. The r_{MeO} data are taken from [7–9].

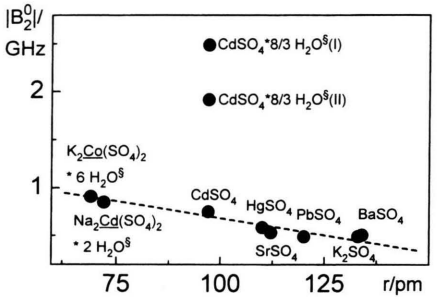

Fig. 7. $|B_2^0|$ at 298 K versus the ionic radii of the host cations. Literature data marked by § were taken from [20]. (I) and (II) for $CdSO_4 \cdot \frac{8}{3} H_2O$ refer to the two crystallographically inequivalent Gd^{3+} sites.

the crystal field strength at the location of the impurity ion. In first approximation this leads to an increase of the ZFS, which is mainly described by the parameter $|B_2^0|$.

However, the cell parameters *a*, *b* and *c* of the host lattices do not show such a clearcut dependence, because their influence on the first ligand sphere (which mainly contributes to the ZFS) is comparably weak.

There exist many examples in the literature where the ZFS shows a clearcut dependence on the ionic radii [18] of the host compound metal ion, e.g., [2, 19]. For Gd^{3+} at the site of the metal atom in this work, the dominant ZFS parameter $|B_2^0|$ appears to decrease linearly with increasing ionic radii as shown in Figure 7. This relationship also applies to $K_2Co(SO_4)_2 \cdot 6H_2O{:}Gd^{3+}$ and $K_2Ni(SO_4)_2 \cdot 6H_2O{:}Gd^{3+}$ [20] which is included in the figure, and where Gd^{3+} occupies the monoclinic site of the divalent metal ion, as well. Here charge compensation is also supposed to take place at larger distances.

Although data are rare, there seems to be a general tendency for monoclinic Gd^{3+} incorporated in sulfates to obey some kind of linear relationship as depicted in Figure 7. Furthermore it is concluded that in monoclinic sulfates which do not obey such a linear tendency, charge compensation takes place in the vicinity of the impurity ion and not at distances. $CdSO_4 \cdot 8/3\,H_2O$, which was measured by Kumaraswamy and Sobhanadri [20], for example, exhibits monoclinic spectra with a ZFS of 1.917 GHz and 2.487 GHz for the two crystallographically inequivalent Cd^{2+} sites. This means a remarkable deviation from the linear tendency stated above, cf. Figure 7.

[1] S. Hansen, D. B. Mosel, and W. Müller-Warmuth, Z. Naturforsch. **51a,** 885 (1996).
[2] J. Kastner, B. D. Mosel, and W. Müller-Warmuth, Z. Naturforsch. **51a,** 1123 (1996).
[3] A. R. Patel and A. L. Bath, J. Cryst. Growth **8,** 153 (1971 a).
[4] A. R. Patel and A. L. Bath, J. Cryst. Growth **11,** 166 (1971 b).
[5] A. R. Patel and J. Kosky, J. Cryst. Growth **2,** 128 (1968).
[6] K. Sahl, Beitr. Mineral u. Petrogr. **9,** 111 (1963).
[7] M. Miyake, I. Minato, H. Morikawa, and S. Iwai, Am. Mineral. **63,** 506 (1978).
[8] A. Aurivilius and C. Stahlhandske, Z. Kristallogr. **153,** 121 (1980).
[9] J. A. McGinnety, Acta Cryst. **B28,** 2845 (1972).
[10] B. Schmitz, M. Jakubith, and G. Lehmann, Z. Naturforsch. **34a,** 906 (1979).
[11] A. Abragam and B. Bleaney. Electron Paramagnetic Resonance of Transition Ions, Clarendon Press, Oxford 1970.
[12] B. V. R. Chowdari and P. Venkateswarlu, J. Chem. Phys. **48,** 318 (1967).
[13] A. D. Rae, J. Chem. Phys. **30,** 2672 (1969).
[14] P. Chand, J. Mathew, A. Punnoose, B. P. Maurya, and R. J. Singh, Spectrochim. Acta, Part A **49A(11),** 1621 (1993).
[15] S. K. Misra and L. E. Misiak, Phys. Rev. B **48, 18,** 13579 (1993).
[16] Y. Y. Yeung and D. J. Newman, J. Phys. C **21,** 537 (1988).
[17] M. W. Walsh, J. Jeener, and N. Bloembergen Phys. Rev. **A139,** 1338 (1965).
[18] Ionic radii from R. D. Shannon, Acta Cryst. **A32,** 751 (1976).
[19] T. Böttjer, G. Lehmann, and M. Stockhausen, Z. Naturforsch. **47a,** 849 (1992).
[20] A. Kumaraswamy and J. Sobhanadri, J. Magn. Res. **31,** 445 (1978).